

EXPERIMENTAL INVESTIGATION ON SURFACE MORPHOLOGICAL BEHAVIOR OF HYDROXYAPATITE COATINGS DEPOSITED OVER METALLIC BIOMATERIAL SURFACES USING PLASMA SPRAY PROCESS

R. B. DURAIRAJ^{a,*}, G. MAGESHWARAN^a, J. JEYAJEEVAHAN^a,
T. ARVIND^b, J. HEMANANDH^a, M. KOK^c

^a*School of Mechanical Engineering, Sathyabama Institute of Science and Technology, Chennai*

^b*Assistant Professor, Department of Mechanical Engineering, Jeppiaar Mamallan Engineering College, Chennai*

^c*Professor, Department of Mechanical Program, Kahramanmaraş Technical Vocational High School, Kahramanmaraş Sütçü İmam University, Turkey*

Metallic biomaterials are of great interest due to their higher mechanical properties. Metallic materials have very high tensile strength, fatigue strength, and fracture toughness as compared to ceramics and polymers. Due to these key properties, metallic materials are the widely used biomaterials for replacing the structural parts of the human body. In this research work, coating of hydroxyapatite has been performed over the metallic biomaterial surfaces using Plasma spray process. The coating expected to form a protective layer over the substrates with good adhesion which helps in achieving improved tissue growth of the implant. The coated samples were examined for surface morphological behavior using Scanning Electron microscope (SEM), Energy dispersive spectroscopy (EDAX) and Fourier – transform infrared spectroscopy (FTIR).

(Received December 23, 2018; Accepted April 17, 2019)

Keywords: Hydroxyapatite, Plasma spray process, Biomaterial, Tissue growth, Surface morphology

1. Introduction

Metallic biomaterials are primarily used in situations where mechanical strength is important. The unique combinations of mechanical properties, such as fatigue strength, toughness and ductility, are essential for structural support in biomedical applications. Titanium and chromium alloys are common. Noble metals provide good corrosion resistance; platinum group metals are used in electrical applications; gold is commonly used in dentistry; and, engineering alloys (titanium and chromium) based on passivated metals provide the passivity. The alloy of cobalt and chromium with varying amounts of molybdenum, nickel and carbon provide a good balance of mechanical properties but their use is limited due to poor ductility (Williams, 1981). Metals and ceramics are more rigid than hard tissues and their use can be counter-intuitive for most tissue replacement. Polymers, on the other hand, show closely similar properties to that of the natural structures. Polymers have wide range of properties from chemical reactivity to mechanical strength, which allows material selection for tailored specification. Polymers are made of macromolecules which are usually nontoxic and hence the use of polymers can have good biocompatibility. However, other substances, such as plasticizers and antioxidants, can add undesirable contaminants tending to reduce or alter the biocompatibility. Polyethylene is suitable for long-term implantation, which is inexpensive and possesses good mechanical properties. The applications of polyethylene range from catheters to joint replacements. In the work of Lee et al. (2000), meta-analysis was performed to resolve the controversy on the reliability of HA coatings

*Corresponding author: durairaj.mech@sathyabama.ac.in

to dental implants. The survival rates of HA coated implants varied from 93.2% to 98.5%, for a period of 4 to 8 years of follow-up, while they varied from 79.2% to 98.5%, for the period of 5 to 8 years of follow-up. The survival rates remained above 90% and showed high reliability of HA coatings in dental implants. Similar work was done by Herrera et al. (2015) and concluded that the HA coated implants showed high survival rates compared to other implants. HA coatings were evaluated on various substrates by research community. HA coating can be done using various coating techniques, such as plasma spraying, pulsed laser-deposition, sputtering, sol-gel, electro-deposition, electrophoresis etc. Among these techniques, electro deposition of HA is regarded as an inexpensive and simple process that can be performed at room temperature. The chemical composition and thickness of HA coating can easily be controlled by appropriately modifying the electro-deposition conditions. The corrosion resistance of HA coating on porous magnesium was investigated by Kang et al. (2013), HA coating was performed by immersing the porous magnesium in the aqueous solution (of ethylenediaminetetraacetic acid calcium disodium salt hydrate and potassium phosphate monobasic in distilled water) for 6 h. The compressive strength increased remarkably from 8 MPa to 17 MPa. It was also found that bio-corrosion of the porous magnesium was inhibited significantly by HA coating. Plasma spraying process is commonly used for HA coatings for fixing implants due to extreme high temperatures. However, they unfortunately degrade easily in a short time after implantation, which may reduce the adhesion of HA layer.

2. Experimental work

2.1. Substrate materials

Three commercially available surgical grade metal substrates (stainless steel, titanium and magnesium alloys) were purchased from the local market near Park Town, Chennai. Stainless steel of SS316L grade, Titanium alloy of Ti6AL4V grade and magnesium alloy of AZ31 grade were purchased as the substrate materials. The materials are so chosen due to their large use in the field of biomedical engineering. These metals have proved their relative mechanical strength in biomedical applications. These materials are considered to be inert in the human body environments.

2.2. Hydroxyapatite preparation

The aqueous solutions of calcium nitrate and diammonium hydrogen phosphate were then transferred to another beaker in which the diammonium hydrogen phosphate solution was added at a flow rate of 3ml/min to form hydroxyapatite solution. The addition of diammonium hydrogen phosphate was done until the pH value reached to 7. At this time, milky white (hydroxyapatite) solution would form. The solution was kept for aging overnight and then dried. The solution was then centrifuged in a cooling centrifuge at 2500 rpm for 15 minutes at 4°C so in order to obtain a sol gel state. It was finally heated in an oven at 80°C and crushed into HA powder. The prepared HA powder was stored in a safe condition.



Fig. 1. Synthesized hydroxyapatite powder.

2.3. Plasma spray

Plasma spray coating is a coating technique that sprays molten or heat-softened material onto a metallic substrate in order to form a coating. The coating material in powder form is injected along with high temperature plasma on to the surface, where the coating material is rapidly heated, allowed to hit the surface at a high velocity and rapidly cooled to form the required coating. In this work, the plasma spray coating was performed at Sathyabama Institute of Science and Technology, Chennai.

2.4. Electrochemical corrosion

Electrochemical corrosion rates were determined with the help of potentiodynamic polarization technique at International Research Centre, Sathyabama University, Chennai. The polarization cell is an experimental setup that consists of electrolyte solution, reference electrode, counter electrode, and working electrode (the metal sample). In this examination, there were three electrodes, (platinum as counter electrode; HA coated Ti6AL4V and SS316 L as the working electrodes and saturated calomel electrode as the reference electrode) used in a polarization cell. These electrodes were immersed in electrolytic solution. SBF solution (100 ml) was used as the electrolyte solution. Square shaped samples (working electrodes) of size of 1cm X 1cm were considered. The sample is attached to a holder. The temperature of 38°C was maintained (which is similar to that of a human body).

Table 1. Parameters for electrochemical corrosion.

Component	Values
Voltage	5 V
Temperature	80° C
Distance	400 mm
Deposition Duration	1 Hour
Cathode	Titanium (Ti)
Anode	Platinum (Pt)

Electrochemical process is actually the combination of oxidation and reduction reactions with the parameter values as mentioned in Table 1. Once corrosion is initiated in the working electrode, electrons are released from the working electrode (oxidation) and attracted (reduction) in the electrolytic solution. The electrodes are attached to potentiostat which is used to control the potential for controlling the polarization scan rate. The scan rate, typically expressed in mV/s, is the rate in which the potential is changed. The scan rate of 0.1667 mV/s is used in the experiment. For electrochemical reactions, the current density is expressed by Tafel equation which is a function of over-potential, $\eta = \beta \log(i/i_0)$, where β is Tafel slope, i the applied current and i_0 the exchange current density. Tafel slope may be obtained from the polarization curve the point, at which the anodic and cathodic reaction rates (i.e., currents) are same, can be calculated. The current density and potential at this point are the corrosion current density (i_{corr}) and the corrosion potential (E_{corr}) respectively. An electrochemical potential is created between the various electrodes with the help of the potentiostat, and the corrosion potential (E_{CORR}) and the corrosion current (I_{CORR}) are recorded. The corrosion current density (i_{CORR}) is combined with Faraday's law as follows: $W = (WA*Q)/(zF)$, where W is the mass of removed material, WA the atomic weight of the samples, Q the total charge (i_{CORR} *time), z the number of electrons and F the Faraday's constant. Once the weight of the removed material is determined, the corrosion rate can then be calculated as, corrosion rate = $(W*As)/\rho$, where As is the exposed surface area and ρ the density.

3. Results and discussion

3.1. Scanning electron microscope

SEM images of HA plasma-sprayed S316L substrates, shown in Fig. 2(a) show that the coating uniformity of HA coating was good and well-distributed over the entire surface. The SEM image at the top showed the appearance of HA plasma-sprayed S316L at low magnification and the SEM image at the bottom showed the appearance of HA plasma-sprayed S316L. From the SEM images, plasma-sprayed HA was observed as the white pigments

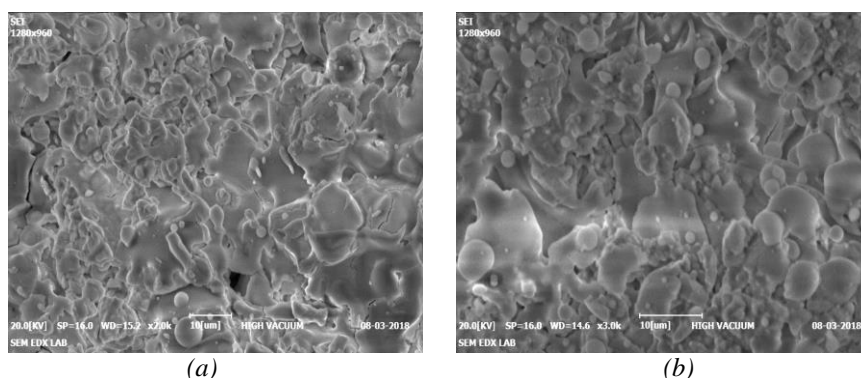


Fig. 1. SEM images of hydroxyapatite coated (a) SS316L (b) Ti6Al4V.

However, as the HA powder was deposited in plasma phase, the adhesion was found to be great and there was visible separation of white patches. As the HA powder was deposited in plasma phase, the adhesion was found to be great. The white regions of HA was observed throughout the S316L substrates and well-distributed. Unlike the HA coating of HA electrodeposited S316L substrates, the adhesion of HA coating was found to be excellent in the case of HA plasma-sprayed S316L substrates. Thus it can be said that plasma-spraying method improved adhesion between the S316L substrates and HA. Therefore, HA plasma-sprayed S316L substrates can effectively be used for improving coating uniformity and adhesion, which can thus be used as an effective biomaterial for implants application with improved characteristics. SEM images of HA plasma-sprayed Ti6Al4V substrates are shown in Fig. 2 (b). The SEM image at the top showed the appearance of HA plasma-sprayed Ti6Al4V at low magnification and the SEM image at the bottom showed the appearance of HA plasma-sprayed Ti6Al4V substrates. The Figure showed that HA coating distributed uniformly throughout the substrate surface. It was important to note that the SEM images did not show the like ball-like objects observed in electro deposition. These ball-like shapes were indicative evidence of the presence of Ti6Al4V in the electro deposition method. However, in the case of HA plasma-sprayed Ti6Al4V substrates, the white pigments of HA coating were observed as simply white patches as seen in S316L biomaterial. Due to plasma spraying, the ball-like structures were not similar to the SEM images observed in electro deposition method. It was also noted that the HA coating was not so well integrated with Ti6Al4V substrates because the white regions were concentrated in some regions, while most of regions consisted of more distributed surface with good adhesion between HA and Ti6Al4V substrates was also great.

3.2. EDAX

The image showed the presence of P, Ca, Mo, Cr, Fe and Ni elements in the HA plasma-sprayed S316L substrates shown in Fig. 3. As S316L contains iron, chromium, Mo and nickel elements in its composition and the resulting EDAX images represent most of these elements, the existence of HA plasma-sprayed S316L substrates was confirmed. HA is made of calcium nitrate and diammonium hydrogen phosphate, and hence the elements such as Ca, O and P were expected as the major elements. EDAX image showed elements of Ca, O and P, which confirms the existence of HA coating. The other minor elements of both S316L and HA were not available for

this particular region. However, the detailed EDAX images, confirmed the presence of most of the elements present in the HA plasma-sprayed S316L substrates. The prepared substrates were therefore confirmed.

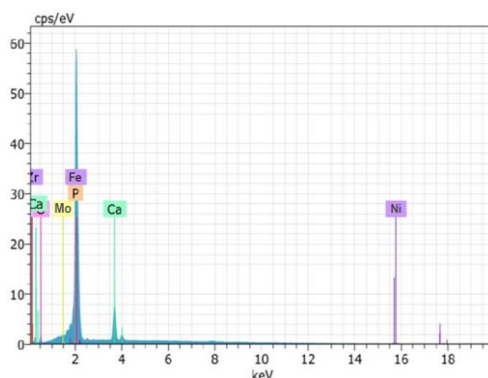


Fig. 3. Edax of HAP coated SS316L.

The image showed the presence of P, Ca, Ti, Al, O and V elements in the HA plasma-sprayed TI-6AL-4V substrates. TI-6AL-4V contains Ti, Al and V as major elements along with other tracing elements and the resulting EDAX images represent most of these elements, which confirmed the existence of HA plasma-sprayed TI-6AL-4V substrates. EDAX image showed elements of Ca, O and P, confirming the existence of HA coating. The other minor elements of both TI-6AL-4V and HA were not available for this particular region. However, the detailed EDAX images, confirmed the presence of most of the elements present in the HA plasma-sprayed TI-6AL-4V substrates. The prepared substrates were therefore confirmed

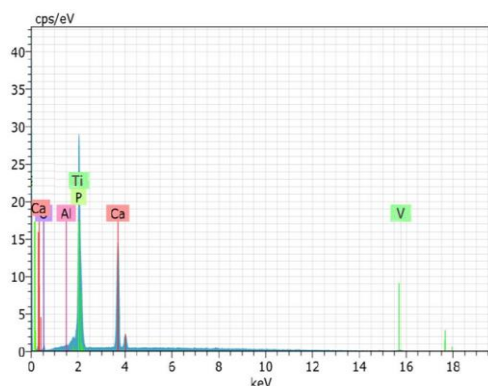


Fig. 4. Edax of HAP coated Ti6AL4V.

3.3. Electrochemical corrosion

Polarization curves of uncoated and HA plasma-sprayed S316L substrates are shown in Fig. 5 The OCR potential of the polarization curve of the HA plasma-sprayed S316L substrates was found to be higher than that of uncoated S316L substrates. This showed that the localized corrosion in the HA plasma-sprayed S316L substrates was initiated later than that of uncoated S316L substrates. It was therefore understood that plasma-spraying of HA was very effective to improve the corrosion resistance in S316L substrates.

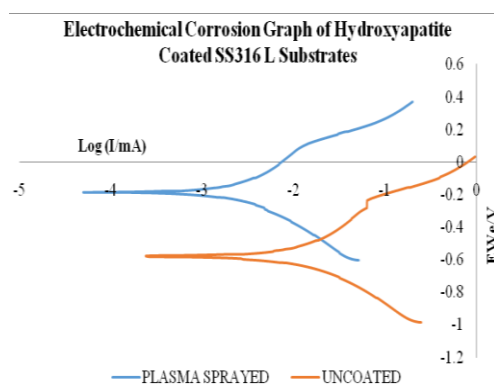


Fig. 5. Polarization curve for hydroxyapatite coated SS316L.

Table 2. Corrosion rates of uncoated and HA plasma sprayed S316L samples

S No	Sample	E_{CORR} (mV)	I_{CORR} (μ A)	Corrosion Rate (mm/year)
1	SS 316 L (Uncoated)	-1252.23	97.31	2.703
2	SS316 L (Plasma Sprayed)	-293.044	8.096	0.0113

Table 2 shows the corrosion potential (E_{corr}), corrosion current (I_{corr}) and corrosion rates of both uncoated and HA plasma-sprayed S316L substrates. E_{corr} of uncoated S316L substrates was -1252 mV, while E_{corr} of HA plasma-sprayed S316L substrates was -293 mV. As E_{corr} of HA plasma-sprayed S316L substrates was higher than that of E_{corr} of uncoated S316L substrates, corrosion potential of HA coated S316L substrates required for producing localized corrosion regions was found to be higher than that of uncoated S316L substrates. This showed that the corrosion initiation was delayed due to the HA coating. The corrosion rates of uncoated and HA plasma-sprayed S316L substrates were 2.703 mm/year and 0.0113 mm/year respectively. Corrosion rate of HA plasma-sprayed S316L substrates was found to be very less than that of the uncoated S316L substrates. From the results, it was found that plasma-spraying of HA improved the corrosion resistance of S316L significantly to a great extent to be very effective for reducing the corrosion in SBF solution.

Table 3 shows the corrosion potential (E_{corr}), corrosion current (I_{corr}) and corrosion rates of both uncoated and HA plasma-sprayed Ti-6Al-4V substrates. E_{corr} and corrosion rates of uncoated Ti6AL4V substrates were 216.25 mV and 0.962 mm/year respectively. E_{corr} and corrosion rates of HA plasma-sprayed Ti6AL4V substrates were 337.67 mV and 0.062 mm/year respectively. Similar to HA plasma-sprayed Ti6AL4V substrates, the corrosion potentials required for producing localized corrosion of HA coated Ti-6Al-4V substrates were found to be higher than that of uncoated Ti-6Al-4V substrates. Corrosion rate of HA plasma-sprayed Ti-6Al-4V substrates was found to be very less than that of the uncoated Ti-6Al-4V substrates. From these results, it could be observed that plasma-spraying of HA improved the corrosion resistance of Ti-6Al-4V.

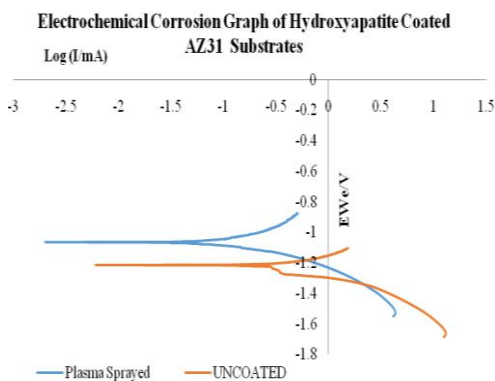


Fig 6. Polarization curve for hydroxyapatite coated Ti6AL4V.

Table 3. Corrosion rates of uncoated and HA plasma sprayed Ti6AL4V samples

S No	Sample	E_{CORR} (mV)	I_{CORR} (μ A)	Corrosion Rate (mm/year)
1	Ti6AL4V (Uncoated)	-420.050	17.886	0.962
2	Ti6AL4V (Plasma Sprayed)	216.25	85.05	0.00801

Fig. 6 shows the polarization curves of uncoated and HA plasma-sprayed Ti-6Al-4V substrates. From the polarization curves, it was found that the OCR potential of the HA plasma-sprayed Ti-6Al-4V substrates was found to be higher than that of uncoated Ti-6Al-4V substrates. The potential required to form the localized corrosion in the HA plasma-sprayed Ti-6Al-4V substrates was higher than that of uncoated Ti-6Al-4V substrates. It was therefore considered to provide excellent corrosion behavior of active corrosion behavior. Therefore, plasma-spraying of HA improved the corrosion resistance in Ti-6Al-4V substrates.

4. Conclusion

Hydroxyapatite coating over SS316L and Ti6AL4V substrates were performed successfully using plasma spray process. The corrosion resistance properties of the coated samples were examined using potentiodynamic polarization examination and the results were listed

Deposition of Hydroxyapatite over Ti6AL4V was found denser when compared to SS316L due to the surface property of the substrate material. It was found very less porous structure in the coated surface of Ti6AL4V due to denser formation of the coating in comparison with SS316L substrate.

The Corrosion rate of SS316L were calculated 0.0113 mm/year of coated surface in comparison with uncoated samples of 2.703 mm/year. The corrosion rate of Ti6AL4V was calculated 0.00801 mm/year of coated surface in comparison with Uncoated Samples of 0.962 mm/year.

Hydroxyapatite coated Ti6AL4V samples shows greater corrosion resistance with SS316L due to major influence of material property and the coating of Hydroxyapatite is able to improve further enhancement of corrosion resistance of the coatings.

References

- [1] Suyalatu, R. Kondo, Y. Tsutsumi, H. Doi, N. Nomura, T. Hanawa, *Acta Biomater* **7**, 4259–4271 (2011).
- [2] A. Szcześ, L. Hołysz, E. Chibowski, *Advances in Colloid and Interface Science* **249**, 321–337 (2017).
- [3] U. I. Thomann, P. J. Uggowitzer, *Wear* **239**, 48 (2000).
- [4] R. C. Thomson, M. J. Yaszemski, J. M. Powers, A. K. Mikos, *Biomaterials* **19**(21), 1935–1943 (1998).
- [5] P. J. Uggowitzer, R. Magdowski, M. O. Speidel, *ISIJ* **36**, 901 (1996).
- [6] H. K. Uthoff, P. Poitras, D. S. Backman, *J. Orthop. Sci.* **11**, 118 (2006).
- [7] S. Vahabzadeh, M. Roy, A. Bandyopadhyay, S. Bose, *Acta Biomaterialia* **17**, 47 (2015).
- [8] M. J. Walter, *Adv. Mater. Process* **164**, 84 (2006).
- [9] G. Y. Wang, P. K. Liaw, Y. Yokoyama, A. Inoue, C. T. Liu, *Mater. Sci. Eng. A* **494**(1), 314–320 (2008).
- [10] K. Wang, *Mat. Sci. Eng. A* **213**, 134 (1996).
- [11] Y. Xin, T. Hu, P. K. Chu, *Acta Biomaterialia* **7**(4), 1452 (2011).
- [12] L. Yi, J. Liu, *International Materials Reviews* **62**(7), 415 (2017).
- [13] L. Zhao, P. K. Chu, Y. Zhang, Z. Wu, *Journal of Biomedical Materials Research Part B: Applied Biomaterials* **91**(1), 470 (2009).
- [14] Y. F. Zheng, X. N. Gu, F. Witte, *Materials Science and Engineering: R: Reports* **77**, 1 (2014).
- [15] R. B. Durairaj, S. Ramachandran, *International Journal of Electrochemical Science* **13**, 4841 (2018).